



## Combined theoretical and experimental studies reveal the newly synthesized pyrimidinones as potential apoptotic agents

Ayaz Mahmood Dar<sup>a,d,\*</sup>, Shafia Mir<sup>b</sup>, Masrat Jan<sup>b</sup>, Rizwan Nabi<sup>e</sup>, Manzoor Ahmad Gatoo<sup>c</sup>, Shamsuzzaman<sup>a,\*</sup>

<sup>a</sup> Department of Chemistry, Aligarh Muslim University, Aligarh 202 002, UP, India

<sup>b</sup> Department of Chemistry, OPJS University, Churu 331001, Rajasthan, India

<sup>c</sup> Department of Biochemistry JNMC, Aligarh Muslim University, Aligarh 202 002, India

<sup>d</sup> Department of Chemistry, Govt. Degree College Kulgam (University of Kashmir), JK, India

<sup>e</sup> Department of Chemistry Indian Institute of Technology Powai Mumbai, 400076, India

### ARTICLE INFO

#### Keywords:

Pyrimidine

DFT

DNA binding, apoptosis

MTT assay

### ABSTRACT

Reaction of acetophenone thiosemicarbazones (5–8) and (2-methyl) diethyl malonate in absolute ethanol under reflux conditions furnished the corresponding pyrimidinone analogs (9–12) in good to excellent yields. The resulting pyrimidines were characterised using spectral and analytical data analysis. The resulting products were studied for DNA interaction studies of by various techniques like UV–VIS, fluorescence spectroscopy, viscosity measurements, molecular docking and gel electrophoresis. To look into the various structural and molecular properties of the target compounds, theoretical DFT involving B3LYP/6-31G\*\* level of theory was employed. Frontier molecular orbital analysis (FMO) was carried out which in turn helped us to determine and evaluate the descriptors like chemical hardness, potential, nucleophilicity and electrophilicity index, etc. Molecular docking and viscosity studies indicated that the synthesized pyrimidinones are minor groove binders of DNA with corresponding intrinsic binding constants of  $3.41 \times 10^3 \text{ M}^{-1}$ ,  $2.91 \times 10^3 \text{ M}^{-1}$ ,  $3.24 \times 10^3 \text{ M}^{-1}$  and  $3.04 \times 10^3 \text{ M}^{-1}$  for compounds (9–12) respectively indicating higher binding affinity of 9 towards DNA. Gel electrophoresis depicted that all new compounds display a dose dependent cleavage activity with pBR322 DNA and efficient nuclease activity was found at 2  $\mu\text{M}$ . An *in vitro* MTT cytotoxicity assay revealed that the compounds (9–12) possess potential toxicity against the different human cancer cells. The AO/EB staining showed that compound 9 caused apoptosis as revealed by the notable apoptotic features like nuclear shrinkage, blebbing and chromatin condensation in HepG2 cells. Compound 9 also caused decrease in the level of apoptotic marker Bcl-XL in Western blotting indicating its prompt ability to cause apoptosis.

### 1. Introduction

Because of the wide spread presence of nitrogen heteroatom in bioactive natural compounds, heteroatom chemistry is emerging as one of the interesting topics in organic synthesis [1]. Pyrimidine derivatives constitute an important class of highly active heterocyclic molecules widely distributed in living organisms [2,3]. Various pyrimidinone derivatives have been prepared with the major substitutions at the C-5 or C-6 position and this process has given birth to potential drugs in chemotherapy [4]. These molecules display numerous biological properties which include antimicrobial [5] antibacterial [6] antitumour [7,8] antiviral [9] antitubercular [10] and antifungal [11,12] activities

and also exist as thyroid drugs [13]. Some biologically important molecules of interest also possess pyrimidine-2-thiol moiety [14]. Carboxamides with pyrimidine moiety have been found to possess notable anticarcinogenic activity [15], antiinflammatory [16] analgesic and blood platelet aggregation inhibitory activity [17]. Numerous drug candidates which include AZD6140 ticagrelor which possesses oral antiplatelet activity [18], HEPT [19] and emivirine (EMV) [20] both of which are 6-substituted uracil derivatives have been chosen as candidates for clinical trials and DABOs [21], potent against HIV-1 synthesis are all embedded with pyrimidinone moiety. Similarly the closely related congeners, dihydropyrimidinones (DHPMs), have also attracted attention because of their notable pharmacological properties and their

\* Corresponding authors at: Department of Chemistry, Aligarh Muslim University, Aligarh 202 002, UP, India (Ayaz Mahmood Dar).

E-mail addresses: [ayazchem@gdckulgam.edu.in](mailto:ayazchem@gdckulgam.edu.in) (A.M. Dar), [shamschem@amu.nic.in](mailto:shamschem@amu.nic.in) (Shamsuzzaman).

<https://doi.org/10.1016/j.comtox.2020.100145>

Received 24 April 2020; Received in revised form 22 September 2020; Accepted 4 November 2020

Available online 7 November 2020

2468-1113/Published by Elsevier B.V.

presence in biologically active natural products [22]. Based on their exceptional biological potential as well as in line with our previous published and recent work [23], we report the synthesis of new pyrimidinone derivatives as metal free DNA binding agents. All the synthesized compounds were characterized by elemental analysis and spectral techniques including IR,  $^1\text{H}$  NMR,  $^{13}\text{C}$  NMR and MS. Various techniques which include UV-vis, fluorescence, gel electrophoresis, viscosity measurements and molecular docking studies were employed to study the binding behaviour of these newly synthesized molecules with DNA, however MTT Assay, confocal microscopy, western blotting and apoptotic studies was carried to study the biological potential of these compounds along with their potential to cause morphological changes in cancer cells, respectively.

## 2. Results and discussion

### 2.1. Chemistry

Synthesis of pyrimidinone derivatives (9–12) was carried out from corresponding thiosemicarbazones (5–8), by refluxing with (2-methyl) diethyl malonate in absolute ethanol as displayed in Scheme 1. The reaction was carried out without the need of harsh reaction conditions. The mechanism for the formation of compounds (9–12) involves the simultaneous nucleophilic attack by the nitrogen atoms of thiosemicarbazone moiety on the carbonyl moieties of the (2-methyl) diethyl malonate eliminating ethoxy [-OEt] groups leading to the formation of products (9–12). The synthesized products were characterized spectral and analytical techniques.

In their IR spectra of compounds (9–12) the presence of absorption bands in the range 3315–3342 shows the presence of NH and as the strong absorption bands at 1675–1679 and 1669–1674  $\text{cm}^{-1}$  confirm the presence of CONH and CON groups, respectively in the compounds (9–12). The absorption bands at 1232–1269 and 1633–1651  $\text{cm}^{-1}$  were ascribed to C = S and C = N groups, respectively. In  $^1\text{H}$  NMR study, the downfield singlet at  $\delta$  7.1–7.6 was ascribed to NH while as the presence of quartet at  $\delta$  3.3–3.6 was assigned to  $-\text{CH}_2-$  proton of pyrimidinone ring. The presence of doublet at  $\delta$  2.2–2.5 was ascribed to for one proton ( $\text{CH}_2-\text{CH}$ ) of the pyrimidinone ring. The  $^1\text{H}$  NMR spectra of the compounds (9–12) also depicted the presence of multiplet in the range of  $\delta$  6.0–6.9 which is ascribed to the aromatic ring protons. In  $^{13}\text{C}$  NMR study, the signals at  $\delta$  184–182, 171.6–172.2, 170.2–172, 158.3–156.4 confirm the presence of C = S, CONH, CON and C = N groups, respectively in the products (9–12). The signals in the range of  $\delta$  124–134 confirm the presence of aromatic ring carbons present in the products (9–12). Finally, the formation of compounds (9–12) was authenticated by the appearance of distinct molecular ion peak  $[\text{M}^+]$  at  $m/z$ : 275, 291, 291 and 307.

### 2.2. DFT studies

After characterizing and validating the structures of the synthesized pyrimidinones we, next studied their reactivity behaviour using theoretical DFT calculations performed at B3LYP/6-31G\*\* level of theory (Fig. S1a and Table S1a, S1b, S2 and S3 in supplementary file). Frontier molecular orbital analysis was carried out using DFT calculations (Fig. 1). HOMO-LUMO energy gap was calculated for all the four products and found to be 0.15, 0.15, 0.15 and 0.15 eV for (9–12) which suggested a similar reactivity nature of compounds in biological interaction. The HOMO-LUMO gap was carried out to assess various reactivity representations of all these molecules which include hardness ( $\eta$ ), potential ( $\mu$ ), electronegativity, electrophilicity which are similar for all the compounds again affirming a similar reactivity profile among them.

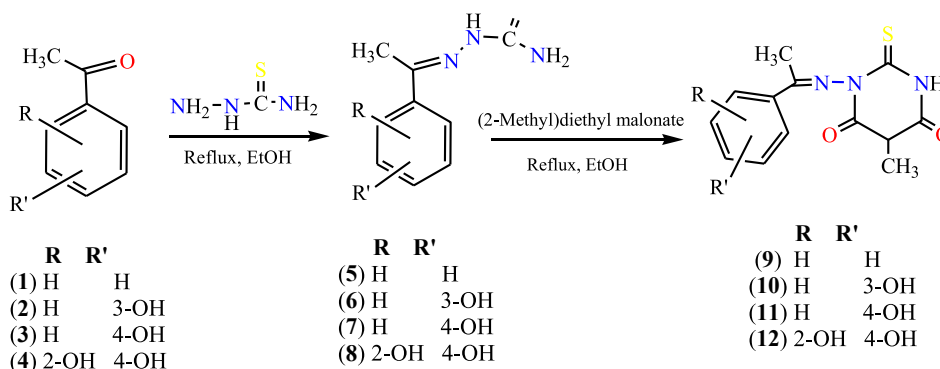
### 2.3. DNA binding

#### 2.3.1. Electronic absorption titration

The UV-vis spectra of compounds (9–12) exhibited intense absorption bands at 340 nm attributed to the  $\pi \rightarrow \pi^*$  or intraligand transitions as shown in Fig. 2. This intense ligand ( $\pi \rightarrow \pi^*$ ) absorption band helps to examine the interaction of the compounds with calf thymus DNA. The absorption intensity of the intraligand absorption band showed a gradual increase with constant increasing concentration of DNA ( $0.70\text{--}4.24 \times 10^{-5}$  M) to the test compounds in 2% DMSO/5mM Tris HCl/50 mM NaCl buffer solution, a process referred as hyperchromism. The observed hyperchromic effect indicates the corresponding conformational and structural changes in DNA [24]. These features suggested that pyrimidines exhibit greater binding tendency with DNA and that too by minor groove interaction involving the phosphate backbone of double helical DNA as well as the hydrophobic interaction. Due to the hydrophobic interactions within the DNA groove, water molecules are being replaced which cause increase in entropy and hence stabilisation of DNA-Molecule complex [25]. Also the binding strength of the synthesized compounds was compared by evaluating their binding constants ( $K_b$ ) derived using the equation below [26].

$$[\text{DNA}]/[\epsilon_a - \epsilon_f] = [\text{DNA}]/[\epsilon_b - \epsilon_f] + 1/K_b[\epsilon_b - \epsilon_f] \quad (1)$$

where, [DNA] represents the concentration of DNA,  $\epsilon_a$ ,  $\epsilon_f$  and  $\epsilon_b$  are the apparent extinction coefficients  $A_{\text{obs}}/[\text{M}]$ , the extinction coefficient for free compound and the extinction coefficient for compound in the fully bound form, respectively. In the plots of  $[\text{DNA}]/\epsilon_a - \epsilon_f$  versus [DNA],  $K_b$  is given by the ratio of the slope to the intercept. The corresponding binding constants for compounds (9–12) were found to be  $3.41 \times 10^3 \text{ M}^{-1}$ ,  $2.91 \times 10^3 \text{ M}^{-1}$ ,  $3.24 \times 10^3 \text{ M}^{-1}$  and  $3.04 \times 10^3 \text{ M}^{-1}$  respectively. The results obtained revealed that compound 9 binds more strongly with CT DNA as compared to the remaining compounds and the binding affinity follows the order  $9 > 11 > 12 > 10$ . Interestingly, the intrinsic



Scheme 1. Schematic representation of synthesis of pyrimidinone (9–12).

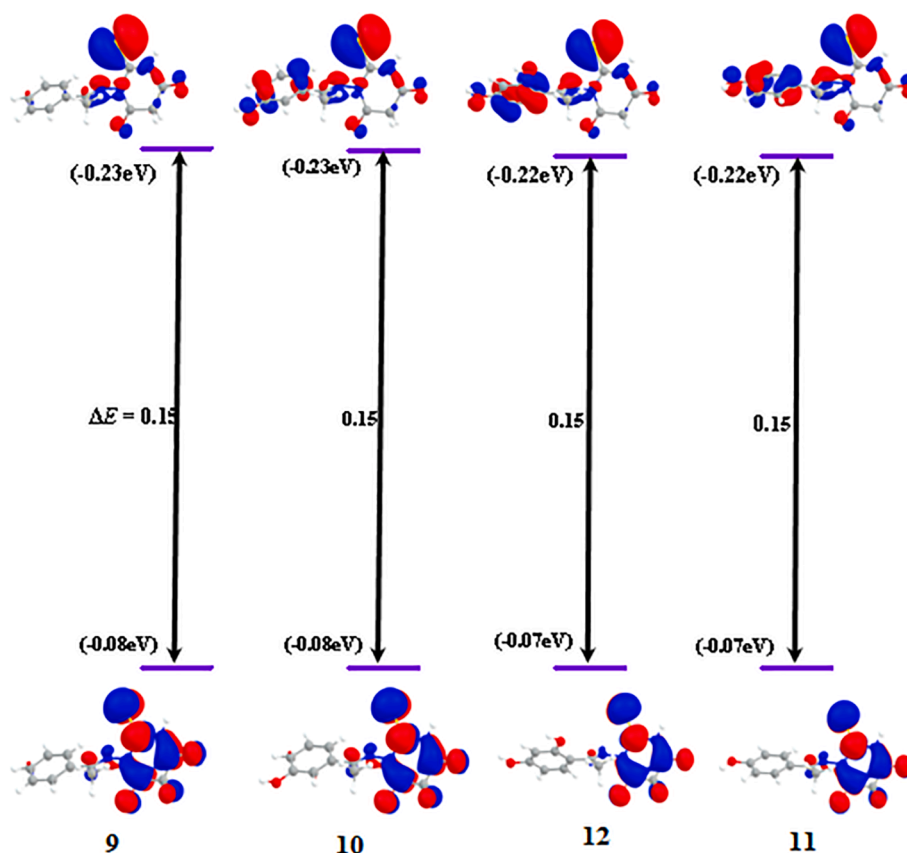


Fig. 1. Selected Highest Occupied Molecular Orbitals (HOMO) and Lowest Unoccupied Molecular Orbitals (LUMO) of 9–12 along with the HOMO-LUMO gap in eV using DFT calculations.

binding  $K_b$  value of compound **9** is higher in magnitude which may be due to the absence of the hindrance or steric reasons by the presence of hydroxyl group (OH) with DNA base pair.

### 2.3.2. Fluorescence spectroscopy

The emission spectra of pyrimidinones (9–12) revealed severe luminescence at 350 nm at room temperature in the absence of DNA when excited at 290 nm. On addition of increasing concentration of DNA ( $0.70 \times 10^{-5}$  to  $4.24 \times 10^{-5}$  M) to the fixed amount of compounds ( $1 \times 10^{-4}$  M), the emission intensity appreciably increases as shown in Fig. 3. The emission intensity largely increases due to the change in environment around molecules. It is also related to the extent to which the molecule is inserted into the hydrophobic environment of DNA. Since DNA is a hydrophobic molecule it reduces the accessibility of solvent molecules to reach the hydrophobic environment inside the DNA helix, and the mobility of the compound is restricted at the binding site ultimately leading to decrease in vibrational mode of relaxation [27]. The binding affinity of compounds was assessed while comparing parameters like binding constant  $K'$  and binding site number 'n' which are calculated using Scatchard equation (2) and (3) [28].

$$C_F = C_T(F/F_o - P) / (1 - P) \quad (2)$$

$$r/c = K(n - r) \quad (3)$$

where,  $C_F$  is the concentration of free compound,  $C_T$  is the total concentration of compound;  $F$  and  $F_o$  are fluorescence intensities in the presence and absence of DNA, respectively.  $P$  is the ratio of observed fluorescence quantum yield of the bound compound to that of the free compound. The value  $P$  was obtained as the intercept by extrapolating from a plot of  $F/F_o$  versus  $1/[DNA]$ ,  $r$  denotes the ratio of  $C_B = (C_T - C_F)$  to the DNA concentration, 'c' is the free compound concentration and 'n' is

the binding site number.

The numerical value of binding constants for the synthesized pyrimidinones (9–12) were found to be  $3.1 \times 10^3 \text{ M}^{-1}$ ,  $2.6 \times 10^3 \text{ M}^{-1}$ ,  $2.8 \times 10^3 \text{ M}^{-1}$ ,  $2.5 \times 10^3 \text{ M}^{-1}$  with corresponding number of binding sites 'n' as 1.54, 1.40, 1.26 and 1.02 respectively. This data revealed that compound **9** has higher DNA binding tendency which is in tune with the electronic absorption titration experiment.

### 2.3.3. Nuclease activity

The DNA cleaving property of pyrimidinones (9–12) was investigated while using pBR322 DNA. Pyrimidinones (9–12) cleaved supercoiled DNA (SC form) (300 ng) in 5 mM Tris-HCl/50 mM NaCl buffer into nicked circular form (NC form) after 1 h of incubation at physiological pH 7.2 and temperature 25 °C. While maintaining the constant concentration of DNA i.e. 300 ng, the concentration of synthesized pyrimidinones (9–12) was varied (1.0–5.0  $\mu\text{M}$ ) and the cleavage process was recorded using gel electrophoresis. The results revealed concentration-dependent electrophoretic cleavage clearly showing the conversion of SC form to NC form with increase in concentration of pyrimidinone (9–12).

All the synthesized pyrimidinones (9–12) exhibited appreciable nuclease activity at 2  $\mu\text{M}$  concentration. However at higher concentrations the SC form transformed itself into NC form completely indicating that the synthesized compounds cause cleavage of double strand DNA (Fig. 4). However when the concentration was further increased, it resulted in the complete uncoiling of double stranded DNA and hence formation of Linear form (LC).

To confirm the interacting site of compound **9** with supercoiled pBR322, both DAPI [29] and methyl green [30] were used. As shown in Fig. 5, only upon adding methyl green (Lane 3) inhibition of the cleavage activity of DNA was observed suggesting that compound **9** has

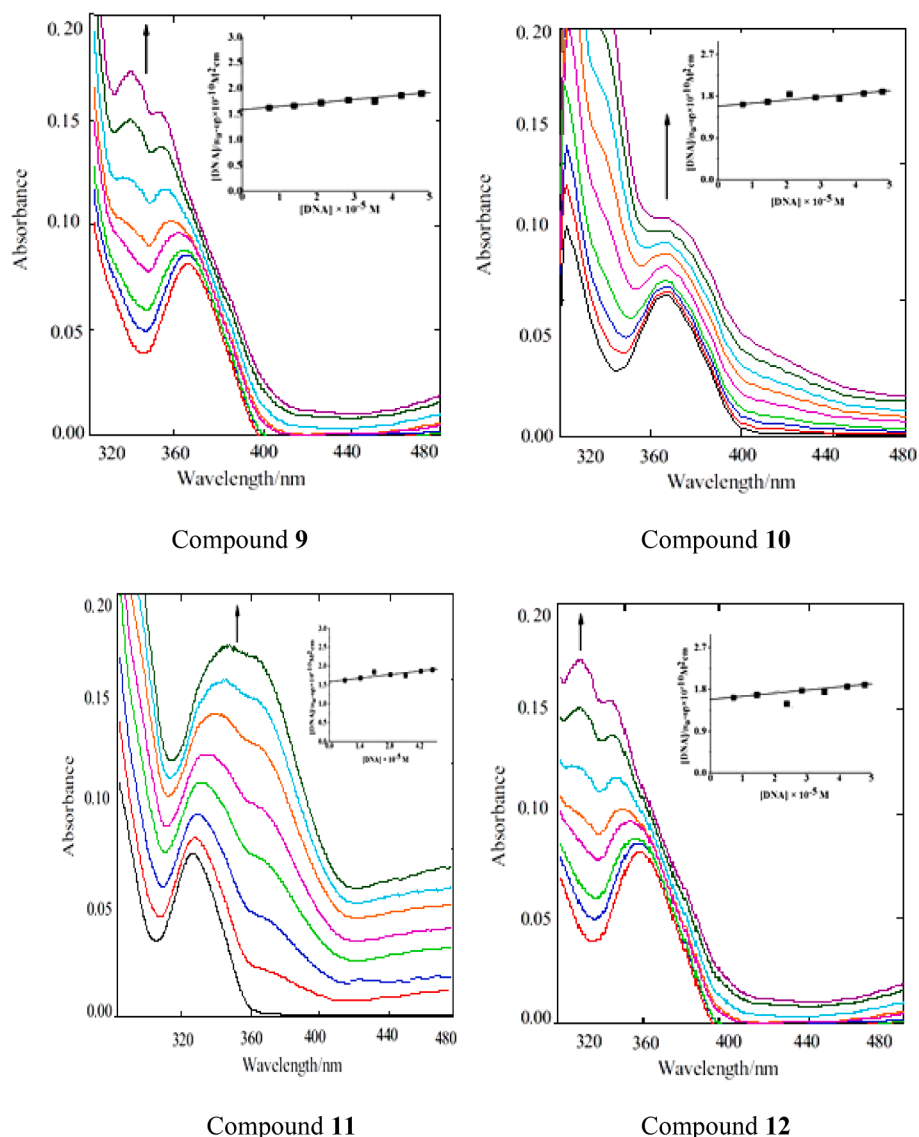


Fig. 2. UV-vis absorption spectra show the variation for compounds (9–12) with increase in the concentration of CT DNA. The arrow shows the change in intensity with increasing DNA concentration.

minor groove binding capability in conformity with many literature reports [31,32].

### 2.3.4. Circular dichroism

The conformation and helicity changes of CT DNA in the presence of the compounds (9–12) were studied using circular dichroism and the results are shown in Fig. 6. Because of the base stacking a positive peak at 275 nm and due to helicity a negative peak at 245 nm was observed [33]. DNA was incubated for 30 min with different concentrations of the compounds (9–12) ( $r([\text{DNA}]/[\text{Compound}]) = 5$  to 1.25). Intensity of both the positive and negative band of DNA has been found to decrease in the presence of the compounds (9–12). However, the change in the intensity of the negative peak is more pronounced than the change in the positive peak intensity. This observation clearly shows that compounds (9–12) affect the helicity of B-DNA.

### 2.3.5. Viscosity measurements

Hydrodynamic properties generally give indications on the binding mode of small molecules with DNA. A plot of relative specific viscosity  $(\eta/\eta_0)^{1/3}$  versus  $[\text{Compound}]/[\text{DNA}]$  where  $\eta$  and  $\eta_0$  are the specific viscosity contribution of DNA in the absence and presence of the

compound, is shown in Fig. 7. As can be seen from the graph, compound 9 showed minor or no variation in the graph [34] suggesting that these compounds interact with CT-DNA via a groove binding mode.

### 2.3.6. Molecular docking studies

Molecular docking technique is an emerging tool to understand the drug-DNA interactions for the rational drug design and discovery, and also in the mechanistic study by placing a small molecule into the binding site of the target specific region of the DNA mainly in a non-covalent fashion, although covalent bond may also be constituted with reactive ligand and to predict the correct binding mode and binding affinities [35]. The Fig. 8 shows favourable docked structures of DNA-Pyrimidinone complex. As can be seen from Fig. 8, these molecules bind to DNA via minor groove such that the OH moiety in three pyrimidinones remains inclined towards the phosphodiester bond of DNA involving themselves in H bonding interactions. It was also found that the resulting binding energy of most favourable docked pyrimidinone–DNA complex is  $-203.81 \text{ kJ mol}^{-1}$ .

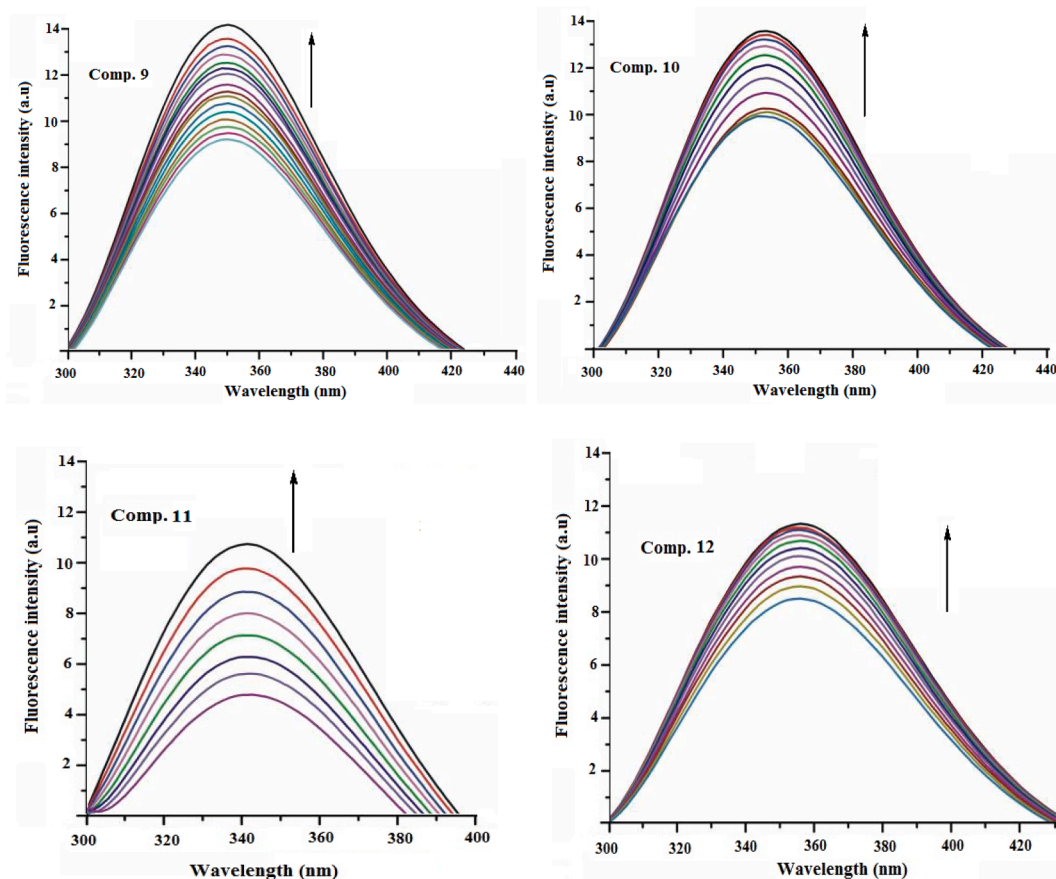


Fig 3. Fluorescence titration of given compounds (9–12) with the CT DNA. Fluorescence intensity increases with subsequent addition of DNA solution.

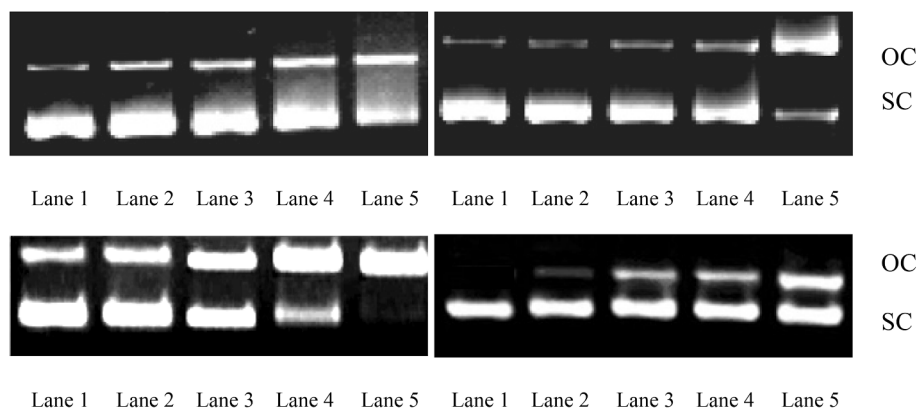


Fig. 4. Agarose gel electrophoresis patterns of pBR322 plasmid DNA (300 ng) cleaved by compound 9–12 (1.0–5.0  $\mu\text{M}$ ), after 1 h incubation time (concentration dependent) Lane 1: control; Lane 2: 1.0  $\mu\text{M}$  9–12 + DNA; Lane 3: 2.0  $\mu\text{M}$  9–12 + DNA; Lane 4: 3.0  $\mu\text{M}$  9–12 + DNA. Lane 5: 4.0  $\mu\text{M}$  9–12 + DNA; Lane 6: 5.0  $\mu\text{M}$  9–12 + DNA in buffer (5 mM Tris-HCl/50 mM NaCl, pH 7.2 at 25  $^{\circ}\text{C}$ ).

#### 2.4. *In vitro* cytotoxicity

The *in vitro* anticancer activity was measured using the MTT assay [36]. Since literature reveals that pyrimidine derivatives being similar to 5-Fluorouracil, a known anticancer drug (which is also pyrimidine derivative) which defines its potentially activeness against different cancer cells, hence with this intuition, a series of pyrimidinone derivatives were synthesized and subsequently *in vitro* anticancer activity was carried out.

During the screening, all the three pyrimidinone derivatives (Table 1) depicted potential anticancer behaviour against given cancer cells by showing less inhibition count particularly compound 9 showed

$\text{IC}_{50}$  8.29  $\mu\text{M}$  and 8.72  $\mu\text{M}$  against MCF-7 and HepG2 cell line, respectively. The compound 10 also revealed potential inhibition i.e. 9.48  $\mu\text{M}$  and 8.33  $\mu\text{M}$  against SW480 and HepG2 cell line, respectively. The inhibition shown by compound 11 was 9.22  $\mu\text{M}$ , 8.87  $\mu\text{M}$  and 9.96  $\mu\text{M}$  against MCF-7, SW480 and HepG2 cell lines, respectively. Compound 12 also showed  $\text{IC}_{50}$  in potential range of 9.62  $\mu\text{M}$  and 11.66  $\mu\text{M}$  against MCF-7 and HepG2 cell line, respectively. The planar and  $\pi$  electron system in aromatic ring of the compound results in higher hydrophobicity which could deeply penetrate into the base pairs of DNA, thereby leading to higher DNA binding tendency. This in turn can lead the DNA damage which causes the growth inhibition of cancer cells.

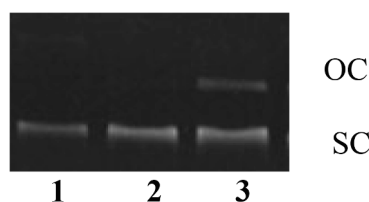


**Fig. 5.** Agarose gel electrophoresis pattern for the cleavage of pBR322 plasmid DNA (300 ng) by **9** (0.25 mmol) Lane 1; DNA control (2.5  $\mu$ L of 0.01 mg/mL solution) Lane 2, DNA + **9** + DAPI (minor groove binding agent); Lane 3, DNA + **9** + methyl green (major groove binding agent); (8 mM), at 310 K after incubation for 45 min.

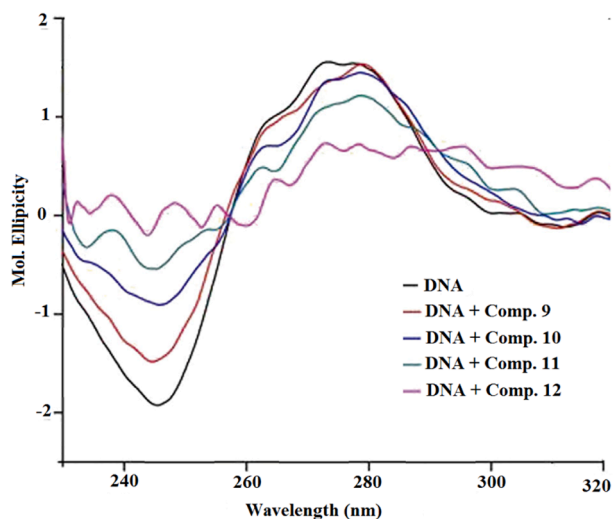


**Fig. 6.** CD spectra of CT DNA in the presence of different compounds (9–12).

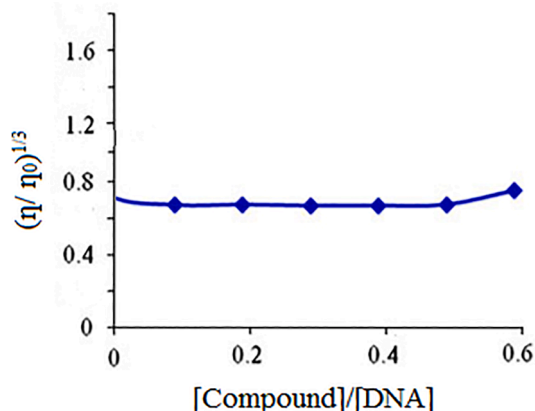


**Fig. 7.** Effect of increasing concentration of compound **9** on the relative viscosities ( $\eta/\eta_0$ ) of CT DNA in Tris-HCl buffer (pH 7.2).

**Fig. 9(A)** shows the photomicrographic images of MCF-7 cells from the control group (no treatment). The micrograph clearly showed a fully confluent growth of cancer cells with prominent nuclei and cytoplasm. **Fig. 9(B) and 9(C)** shows treatment of MCF-7 cells with compound **9** for 36 h and 48 h and it was observed that a considerable growth inhibition in cell proliferation was observed. It demonstrated the apoptotic characteristic in the cells with some important apoptosis features such as the cell shrinkage, membrane blebbing, nuclear-condensation and apoptotic bodies in cytoplasm. The cancer cells treated with the standard drug have been shown in **Fig. 9D**. The standard drug (5-FU) caused enormous cytotoxicity as the proliferation of the cells affected with significant

cellular changes. The photomicrograph depicts clearly that compound **9** affected the basic morphology of most of MCF-7 cells them to lose viability.

### 2.5. Apoptosis by AO/EB staining method

AO can pass the cell membrane of living or early apoptotic cells, while staining by EB indicates loss of membrane integrity. Under a fluorescence microscope, living cells appear green, necrotic cells stain red but have a nuclear morphology resembling that of viable cells. In the control, the living cells are stained bright green in spots. After treatment of HepG2 cells with 10  $\mu$ M of compound **9** and **10** for 24 h, the green apoptotic cells with apoptotic features such as nuclear shrinkage, chromatin condensation, as well as red necrotic cells, were observed (**Fig. 10**).

### 2.6. Western blot analysis

To confirm the apoptotic effect of compound **9** in MCF-7 cells, a study of protein levels of some apoptotic markers such as Caspase-3, Bax, Bcl-XL and PARP cleavage was performed by Western blot analysis (**Fig. 11**). The expression of Bcl-XL was reduced when cells were exposed to compound **9** of increasing concentrations (0, 10, 15 and 20  $\mu$ M). In contrast to Bcl-XL, the expression of Bax and Caspase-3 was increased.

The level of cleaved PARP product (104 KDa) was higher in the treated cells than untreated cells and increased with increasing concentrations of the compound **9**. As expected, the expression of  $\beta$ -actin, which served as a loading control, remained unaltered. These relative expressions of relevant apoptotic markers including the increasing Bax/Bcl-XL ratio, Caspase-3 and PARP cleavage clearly indicate that compound **9** causes apoptosis in MCF-7 cancer cells.

## 3. Experimental

### 3.1. Materials and methods

All the melting points were determined in degrees Celsius on a Kofler apparatus and are uncorrected. The IR spectra were recorded with KBr pellets on Perkin Elmer RXI spectrophotometer and values are given in  $\text{cm}^{-1}$ .  $^1\text{H}$  and  $^{13}\text{C}$  NMR spectra were run in  $\text{CDCl}_3$  on a JEOL Eclipse (400 MHz) instrument with TMS as internal standard and values are given in ppm ( $\delta$ ). Mass spectra were recorded on a JEOL SX 102/DA-6000 Mass Spectrometer. Thin layer chromatography (TLC) plates were coated with silica gel G and exposed to iodine vapours to check the homogeneity as well as the progress of reaction. All the chemicals were purchased from Merck India. Super coiled pBR322 DNA was purchased from GeNei (India) while as double-stranded calf thymus DNA, purchased from Sigma, was dissolved in a 0.1 M Tris-buffer. The purity of DNA was verified by monitoring the ratio of absorbance at 260 nm to that at 280 nm, which was in the range 1.8–1.9. The DNA concentration was spectrophotometrically determined using  $\epsilon_{260} = 6600 \text{ M}^{-1} \text{ cm}^{-1}$  [37]. The human cancer cell lines used for the cytotoxicity experiment were MCF-7, HeLa, HL-60, SW480 and HepG2 which were obtained from the National Cancer Institute (NCI), biological testing branch, Frederick Research and Development Centre, USA.

### 3.2. General method for the synthesis of acetophenone thiosemicarbazone (5–8)

The known acetophenone thiosemicarbazone (5–8) were synthesized by a literature method [38] which involves the refluxing of an equimolar solution of acetophenone and its derivatives (1–4) and thiosemicarbazide in ethanol in the presence of few drops of HCl for 3 h. After cooling, the compounds were filtered and purified by recrystallization from methanol.

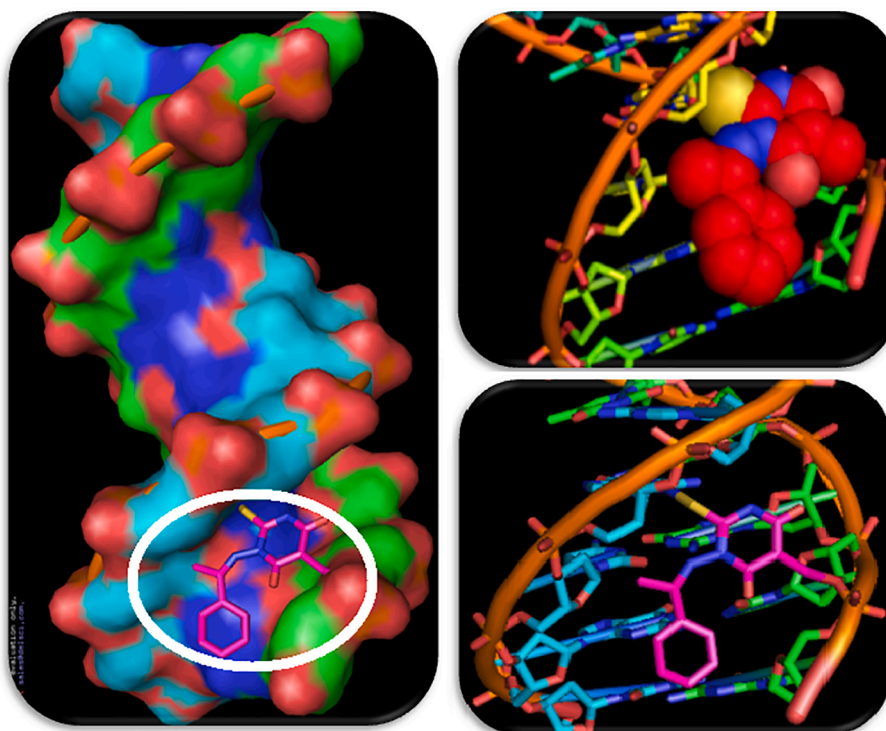


**Fig. 8.** Cartoon representation of DNA with the bound compound **9**. The N-, S- and the O- termini of the compound are shown as blue, yellow and red sticks, respectively. The white encircled area shows the orientation of compound in minor groove of DNA with minimum energy poses in terms of ball stick and sphere models. (For interpretation of the references to colour in this figure legend, the reader is referred to the web version of this article.)

**Table 1**

MTT assay showing the IC<sub>50</sub> values by **9–12**, Cisplatin and 5-Fu against given panel of cancer cell lines.

IC <sub>50</sub> (μM)					
	Breast	Cervical	Leukemia	Colon	Hepatic
Comp	MCF-7	HeLa	HL-60	SW480	HepG2
<b>9</b>	<b>8.29</b>	12.62	15.78	10.33	<b>8.72</b>
<b>10</b>	11.31	10.38	13.91	<b>9.48</b>	<b>8.33</b>
<b>11</b>	9.22	10.66	14.42	8.87	9.96
<b>12</b>	12.43	11.77	9.62	13.32	11.66
5-FU	8.4	7.32	6.45	9.71	7.31
Cisplatin	6.23	5.21	5.83	4.62	5.78

5-FU = 5-Fluorouracil.

### 3.3. General method for the synthesis of pyrimidinones (**9–12**)

To a solution of acetophenone thiosemicarbazone and its derivatives (**5–8**) (1.5 mmol) in absolute ethanol (20 mL), an equimolar amount of (2-methyl) diethyl malonate was added. The reaction mixture was refluxed for 5 h. The progress and completion of the reaction was

monitored by TLC. After completion of reaction, the excess solvent was reduced to three fourths of the original volume under reduced pressure. The reaction mixture was then taken in ether, washed with water and dried over anhydrous sodium sulfate. Evaporation of solvents and crystallization from methanol afforded the corresponding pyrimidinones (**9–12**).

#### 3.3.1. 5-Methyl-1-(1'-phenylethylidamino)-2-thioxo-dihydropyrimidin-4, 6-dione (**9**)

Yield 72%; m.p. 155 °C; Analysis found: C, 53.56, H, 4.37, N, 14.31%. C<sub>13</sub>H<sub>13</sub>N<sub>3</sub>O<sub>2</sub>S requires: C, 53.60, H, 4.50, N, 14.42%; IR (KBr):  $\nu_{\max}$  3322 (NH), 1677 (CONH), 1670 (CON), 1651 (C=N), 1232 (C=S), 1025 (C-N); <sup>1</sup>H NMR (CDCl<sub>3</sub>):  $\delta$  7.6 (s, 1H, NH, exchangeable with D<sub>2</sub>O), 6.4–6.9 (m, 5H, aromatic), 3.6 (q, 1H, C<sub>5'</sub>H), 2.3 (d, 3H, CH<sub>3</sub>); <sup>13</sup>C NMR (CDCl<sub>3</sub>):  $\delta$  182 (C<sub>2</sub>), 172.1 (C<sub>4</sub>), 171.2 (C<sub>6</sub>), 153.3 (C<sub>1'</sub>), 52.2 (C<sub>5</sub>), 124–132 (6 aromatic carbons); MS:  $m/z$  275 [M<sup>+</sup>].

#### 3.3.2. 5-Methyl-1-(1'-(3''-hydroxyphenyl)-ethylidamino)-2-thioxo-dihydropyrimidin-4, 6-dione (**10**)

Yield 70%; m.p. 172 °C; Analysis found: C, 53.60, H, 4.50, N, 14.42%. C<sub>13</sub>H<sub>13</sub>N<sub>3</sub>O<sub>3</sub>S requires: C, 53.56, H, 4.38, N, 14.35%; IR (KBr):

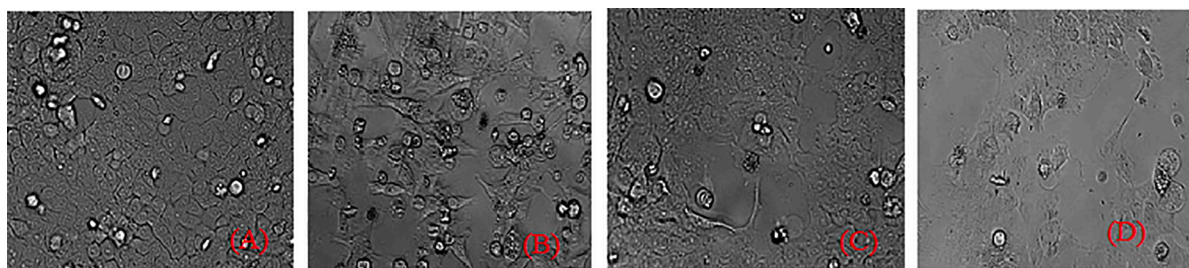


**Fig. 9.** MCF-7 cell images were taken under an inverted phase-contrast microscope with a digital camera at 48 h after treatment with the compound **9**. The images depict (A) Control, (B) Compound **9** after 36 h treatment, (C) Compound **9** for 48 h treatment and (D) treatment with 5-Fu.

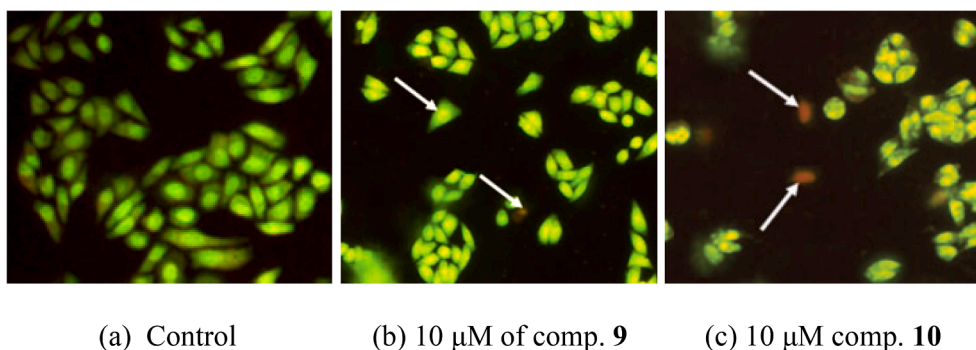


**Fig. 10.** HepG2 cells were stained by acridine orange (AO) / ethidium bromide (EB) and observed under fluorescence microscopy. (a) Control, (b) exposure to 10  $\mu\text{M}$  of compound 9 and (c) exposure to 10  $\mu\text{M}$  of compound 10 incubated at 37  $^{\circ}\text{C}$  and 5%  $\text{CO}_2$  for 24 h. (For interpretation of the references to colour in this figure legend, the reader is referred to the web version of this article.)

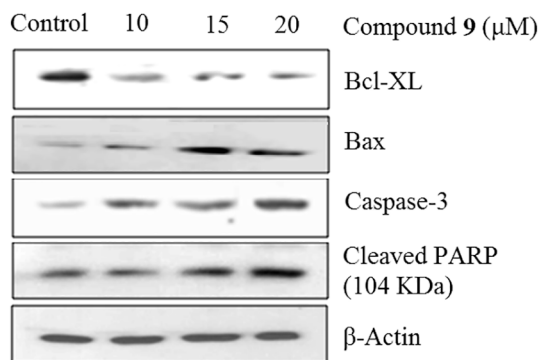


**Fig. 11.** Western blot analysis of whole cell extracts. Lower panel ( $\beta$ -actin) represent equal loading of each lane.

$\nu_{\text{max}}$  3412 (OH), 3342 (NH), 1679 (CONH), 1674 (CON), 1643 (C = N), 1269 (C = S), 1080 (C-O), 1025 (C-N);  $^1\text{H}$  NMR ( $\text{CDCl}_3$ ):  $\delta$  7.9 (s, 1H, OH, exchangeable with  $\text{D}_2\text{O}$ ),  $\delta$  7.1 (s, 1H, NH, exchangeable with  $\text{D}_2\text{O}$ ),  $\delta$  6.5–6.1 (m, 4H, aromatic), 3.5 (q, 1H,  $\text{C}_5'$ -H),  $\delta$  2.3 (d, 3H,  $\text{CH}_3$ );  $^{13}\text{C}$  NMR ( $\text{CDCl}_3$ ):  $\delta$  183 ( $\text{C}_2$ ), 171.6 ( $\text{C}_4$ ), 170.2 ( $\text{C}_6$ ), 158.3 ( $\text{C}_1'$ ), 52.2 ( $\text{C}_5$ ), 127–134 (6 aromatic carbons); MS:  $m/z$  291 [ $\text{M}^+$ ].

### 3.3.3. 5-Methyl-1-(1'-(4-hydroxyphenyl)-ethylidnamino)-2-thioxo-dihydropyrimidin-4, 6-dione (11)

Yield 73%; m.p. 185  $^{\circ}\text{C}$ ; Analysis found: C, 53.60, H, 4.50, N, 14.4%.  $\text{C}_{13}\text{H}_{13}\text{N}_3\text{O}_3\text{S}$  requires:

C, 53.54, H, 4.39, N, 14.30%; IR (KBr):  $\nu_{\text{max}}$  3418 (OH), 3315 (NH), 1675 (CONH), 1671 (CON), 1637 (C = N), 1254 (C = S), 1080 (C-O), 1025 (C-N);  $^1\text{H}$  NMR ( $\text{CDCl}_3$ ):  $\delta$  8.2 (s, 1H, OH, exchangeable with  $\text{D}_2\text{O}$ ),  $\delta$  7.6 (s, 1H, NH, exchangeable with  $\text{D}_2\text{O}$ ),  $\delta$  6.2–6.4 (m, 4H, aromatic), 3.5 (q, 1H,  $\text{C}_5'$ -H),  $\delta$  2.4 (d, 3H,  $\text{CH}_3$ );  $^{13}\text{C}$  NMR ( $\text{CDCl}_3$ ):  $\delta$  184 ( $\text{C}_2$ ), 172.1 ( $\text{C}_4$ ), 171.2 ( $\text{C}_6$ ), 157.3 ( $\text{C}_1'$ ), 59.6 ( $\text{C}_5$ ), 127–134 (6 aromatic carbons); MS:  $m/z$  291 [ $\text{M}^+$ ].

### 3.3.4. 5-Methyl-1-(1'-(2'', 4''-dihydroxyphenyl)-ethylidnamino)-2-thioxo-dihydropyrimidin-4,6-dione (12)

Yield 68%; m.p. 187  $^{\circ}\text{C}$ ; Analysis found: C, 50.75, H, 4.19, N, 13.59%.  $\text{C}_{13}\text{H}_{13}\text{N}_3\text{O}_4\text{S}$  requires: C, 50.81, H, 4.26, N, 13.67; IR (KBr):  $\nu_{\text{max}}$  3426 (OH), 3325 (NH), 1677 (CONH), 1669 (CON), 1633 (C = N), 1249 (C = S), 1072 (C-O), 1036 (C-N);  $^1\text{H}$  NMR ( $\text{CDCl}_3$ ):  $\delta$  8.2, (s, 1H, OH, exchangeable with  $\text{D}_2\text{O}$ ), 8.0 (s, 1H, OH, exchangeable with  $\text{D}_2\text{O}$ ),  $\delta$  7.4 (s, 1H, NH, exchangeable with  $\text{D}_2\text{O}$ ),  $\delta$  6.0–6.3 (m, 3H, aromatic), 3.3 (q, 1H,  $\text{C}_5'$ -H<sub>2</sub>),  $\delta$  2.6 (d, 3H,  $\text{CH}_3$ );  $^{13}\text{C}$  NMR ( $\text{CDCl}_3$ ):  $\delta$  184 ( $\text{C}_2$ ), 172.2 ( $\text{C}_4$ ), 172 ( $\text{C}_6$ ), 156.4 ( $\text{C}_1'$ ), 58.4 ( $\text{C}_5$ ), 127–134 (6 aromatic carbons); MS:  $m/z$  307 [ $\text{M}^+$ ].

## 3.4. DNA binding studies

### 3.4.1. Absorption and emission spectroscopy

The DNA binding experiments were carried out by using absorption titration and emission spectroscopy as reported in literature [39]. The UV-vis spectra for DNA compound (9–12) interactions were obtained using an Agilent 8453 spectrophotometer while as fluorescence measurements were carried out with a JASCO spectrofluorimeter (FP 6200). Solutions of DNA and compound (9–12) were scanned in a 1 cm quartz cuvette. To eliminate the absorbance of the DNA while measuring the absorption spectra, an equal amount of DNA was added to both the compound solution and the reference solution.

### 3.4.2. Nuclease activity

Cleavage experiments were performed with the help of Axygen electrophoresis supported by Genei power supply with a potential range of 50–500 V, visualized and photographed by Vilber-INFINITY gel documentation system. Cleavage experiments of supercoiled pBR322 DNA (300 ng) by compounds 9–12 (1.0–5.0  $\mu\text{M}$ ) in (5 mM Tris-HCl/50 mM NaCl), buffer at pH 7.2 were carried out and the reaction followed by agarose gel electrophoresis. The samples were incubated for 1 h at 37  $^{\circ}\text{C}$ . A loading buffer containing 25% bromophenol blue, 0.25% xylene cyanol and 30% glycerol was added and electrophoresis was carried out at 60 V for 1 h in Tris-HCl buffer using 1% agarose gel containing 1.0  $\mu\text{g}/\text{mL}$  ethidium bromide [40]. The reaction was also monitored upon addition of groove binders-MG and DAPI.

### 3.4.3. Circular dichroism

CD spectra of CT DNA (200 mM) were analysed in the absence and presence of increasing concentration of compounds. Spectra were run for R values 5, 2.5, 1.6 and 1.25 ( $R = \frac{1}{2} [\text{DNA}]/[\text{compound}]$ ). CD spectra were taken as the average of three independent scans between 220 and 330 nm using JASCO J-815CD spectrometer with 150 W Xenon arc lamp.

### 3.4.4. Viscosity measurements

Viscosity measurements [41] were made using a viscometer (SCHOTAVS 450) which was maintained at temperature  $25 \pm 0.5$   $^{\circ}\text{C}$  using a constant temperature bath. The DNA concentration was fixed at  $5 \times 10^{-5}$  M and flow time was measured with a digital stopwatch; the mean values of three replicated measurements were used to evaluate the viscosity ( $\eta$ ) of the compound. The data were reported as  $(\eta/\eta_0)^{1/3}$  versus the [Compound]/[DNA] ratio (ri), where  $\eta_0$  is the viscosity of the DNA solution alone.

### 3.4.5. Molecular docking

The rigid molecular docking studies were performed using HEX 6.1 software [42]. The compound 9 was taken for the following docking

study. The crystal structure of the B-DNA dodecamer d(CGCAAAATTCGC)<sub>2</sub> (PDB ID : 1BNA) was downloaded from the protein data bank. All calculations were carried out on an Intel CORE i5, 3.1 GHz based machine running MS Windows XP as the operating system. First of all the water molecules were deleted. The DNA was enclosed in a box with number of grid points in x × y × z directions, 76 × 78 × 120 and a grid spacing of 0.375 Å. Visualization of the docked pose have been done using Discovery Studio 3.5 molecular graphics program.

### 3.5. *In vitro* cytotoxicity

To study the cytotoxic effect of the compounds, *in vitro* MTT assay was carried out [36]. Human cancer cell lines SW480 (colon adenocarcinoma cells)/ATCC (CCL-228), HeLa (cervical cancer cells)/ATCC (CCL-2), MCF-7 (breast cancer cells)/ATCC (HTB-22), HepG2 (hepatic carcinoma cells)/ATCC (CRL-8065) and HL-60 (Leukaemia cells)/ATCC (CCL-240) were taken for the study. SW480, HL-60 and HepG2 cells were grown in RPMI 1640 supplemented with 10% foetal bovine serum (FBS), 10U penicillin and 100 µg/mL streptomycin at 37 °C with 5% CO<sub>2</sub> in a humidified atmosphere. HeLa and MCF7 cells were grown in Dulbecco's modified Eagle's medium (DMEM) supplanted with FCS and antibiotics as described above for RPMI 1640. The cells were incubated in an incubator at 37 °C and 5% CO<sub>2</sub>. After 24 h, the cells were serum starved overnight. Compounds 9–12 were then added prepared in DMSO in a concentration range of 3–100 µM, ensuring an equal volume of 200 µL across the wells of the plate. The plate was further incubated at 37 °C and 5% CO<sub>2</sub> for 48 h. The cytotoxicity of the compounds was tested by the addition of the yellow tetrazolium salt MTT (3-(4,5-dimethylthiazolyl-2)-2,5-diphenyltetrazoliumbromide) prepared in culture medium at a working concentration of 0.4 mg/mL across the plate. The plate was further incubated for 2 h so that MTT is reduced by the live cells, to produce a purple Formazan product. After this time, the medium was aspirated and 200 µL of DMSO (Sigma Ltd.) was added to each well. The experiment was performed in triplicates. The plate was agitated gently for 5 min. before measuring the optical density at 570 nm in each well using Thermo Scientific multi-plate reader (MultiSkan EX Elisa reader). Since the absorbance correlated with the number of viable cells the percentage of viability was calculated from the absorbance. The IC<sub>50</sub> values of the compounds were determined by plotting the percentage viability versus concentration on a logarithmic graph and the reading of the concentration at which 50% of cells are viable relative to the control.

### 3.6. Apoptosis studies with (AO)/ (EB) staining method

Apoptotic studies were performed with a staining method utilising Acridine Orange (AO) and Ethidium Bromide (EB) [43]. A monolayer of HepG2 cells was incubated in the absence or presence of compounds 9 and 10 at concentration of 10 µM at 37 °C and 5% CO<sub>2</sub> for 24 h. Each cell culture was then stained with AO/EB solution (100µg mL<sup>-1</sup> AO, 100µg mL<sup>-1</sup> EB). The cell cultures were observed under a fluorescence microscope.

### 3.7. Western blot analysis

MCF-7 cells were grown on 100 mm tissue culture discs at a density of 1 × 10<sup>6</sup> cells per plate and incubated overnight. Then the cells were exposed to compound 9 (0, 10, 15 and 20 µM) for 48 h prior to harvest. The cell lysate was prepared by using modified RIPA lysis buffer (50 mM tris, 150 mM NaCl, 0.5 mM deoxycholate, 1% NP-40, 0.1% SDS, 1 mM Na<sub>3</sub>VO<sub>4</sub>, 5 mM EDTA, 1 mM PMSF, 2 mM DTT, 10 mM β-glycerophosphate, 50 mM NAF, 0.5% triton X-100, protease inhibitor cocktail). Protein estimation was done by Bradford's method. Proteins were separated in 10% SDS-PAGE and transferred to Peripheral vascular disease membrane. Membranes were blocked overnight in 10% skimmed milk in 1 × TBS-T (Tris-buffered saline containing 0.05% of Tween-20)

at 4 °C and immunoblotted with antibodies anti-Bcl-XL, anti-Bax and anti-PARP. Detection of signals was done using ECL Western blotting reagent and chemiluminescence was exposed on Kodak X-Omat films. Antibody anti-β-actin was used as loading control. All the antibodies were procured from cell signalling technology, CA, USA.

### 3.8. Computational details

All the DFT calculations were performed using the Gaussian 09 code [44]. B3LYP functional was employed for the optimization of all the structures [45]. The B3LYP functional is believed to yield the correct structures [46]. The geometry optimization was carried out using a 631G\*\* basis set for all the atoms. All structures studied in this work were fully optimized in gas-phase without any restriction.

## 4. Conclusion

In conclusion, we have synthesized and characterized pyrimidinone derivatives. DFT studies revealed a similar reactivity pattern of these compounds as deduced from the similar HUMO-LUMO energy gap of all the synthesized pyrimidinones. Spectroscopic titration revealed that compounds (9–12) are minor groove binders. The absorption and fluorescence studies reveal the stabilization of the energy levels of the compounds in the presence of DNA. *In vitro* cytotoxicity screening revealed that pyrimidinones are potential cytotoxic agents against the cancer cell lines. These relative expressions of relevant apoptotic markers including the increasing Bax/Bcl-XL ratio, cleaved Caspase-3 and PARP cleavage clearly indicated that these pyrimidinones have prompt ability to cause apoptosis. In short, this study reveals that these semi-synthesized pyrimidinones can be used as template for future drug development through even different derivatization to prepare more potent and selective-DNA binding agents.

### CRediT authorship contribution statement

**Ayaz Mahmood Dar:** Conceptualization, Supervision, writing. **Shafia Mir:** Data Curation, Investigation. **Masrat Jan:** Methodology, Resources, Visualization. **Rizwan Nabi:** Software, Visualization, Validation, Formal Analysis, Funding acquisition. **Manzoor A Gatoor:** Project administration, review and editing.

### Declaration of Competing Interest

The authors declare that they have no known competing financial interests or personal relationships that could have appeared to influence the work reported in this paper.

### Acknowledgments

The Author (AMD) also thanks University Grants Commission India for JRF/SRF and for successful completion of work. The authors (MJ and SM) thank the Department of Chemistry OPJS University for completion of this work. The corresponding author also thanks MAG for successful biological studies. We are greatly thankful to G. Rajaraman IIT Bombay for providing computational facility.

### Appendix A. Supplementary data

Supplementary data to this article can be found online at <https://doi.org/10.1016/j.comtox.2020.100145>.

### References

- [1] (a) S. Kumar, M. Ceruso, T. Tuccinardi, C.T. Supuran, P.K. Sharma, Pyrazolylbenzo imidazoles as new potent and selective inhibitors of carbonic anhydrase isoforms hCA IX and XII, *Bioorg. Med. Chem.* 24 (2016) 2907–2913.

- [2] a) M.A. El-Agrody, M.F. Ali, A.F. Eid, A.A.M. El-Nassag, G. ElSherbeny, H.A. Bedair, Phosphorus Sulfur and Silicon, 2006, 181, 839; b) A.R. Katritzky, Advances in Heterocyclic Chemistry (Academic Press, New York, 1966), Vol. 6. Thioxopyrimidines and Related Derivatives 863; c) C.R. Criag, E.F. Shidenman, J. Pharmacol. Exp. Ther., 35 (1971) 179; Chem. Abstr., 74, 62990j (1971). d) D.T. Hurst, J.C. Christophides, Heterocycles 6, 1977 (1999).
- [3] K.M. Ghoneim, R. Youssef, J. of Indian Chem. Soc. 53 (1986) 914.
- [4] a) F.J. Giles, Expert Rev. Anticancer Ther. 2 (2002) 261; b) S. Knapp, Chem. Rev. 1995 (1859) 95; c) K. Felczak, A.K. Drabikowska, J.A. Vilpo, T. Kulikowski, D. Shugar, J. Med. Chem. 39 (1996) 1720.
- [5] B.K. Karale, C.H. Gill, M. Khan, V.P. Chavan, A.S. Mane, M.S. Shingare, Indian J. Chem.-Section B: Org. Med. Chem. 9(41B) (2002) 1957.
- [6] S.N. Thore, Oriental J. Chem. 22 (2006) 651.
- [7] V.M. Reddy, G.V.S. Sarma Rama, Indian J. Heterocyclic Chem. 3 (1993) 111.
- [8] a) G.M. Szczeczek, P. Furman, G.R. Painter, D.W. Barry, K. BorrotoEsoda, T.B. Grizzle, M.R. Blum, J.P. Sommadossi, R. Endoh, T. Niwa, M. Yamamoto, C. Moxham, Antimicrob. Agents Chemother. 44 (2000) 123; b) F.J. Giles, E.J. Feldman, G.J. Roboz, R.A. Larson, S.W. Mamus, J.E. Cortes, S. Verstovsek, S. Federl, M. Talpaz, M. Beran, M. Albitar, S.M. O'Brien, H.M. Kantarjian, Leuk. Res. 27 (2003) 1091; c) F. Giles, J. Expert Rev. Anticancer Ther. 2 (2002) 261; d) J. Toyohara, A. Hayashi, M. Sato, 91 A. Gogami, H. Tanaka, K. Haraguchi, Y. Yoshimura, H. Kumamoto, Y. Yonekura, Y. Fujibayashi, Nucl. Med. Biol. 30 (2003) 687; e) T.J. Mangner, R.W. Klecker, L. Anderson, A.F. Shields, Nucl. Med. Biol. 30 (2003) 215. (f) J. Toyohara, Y. Fujibayashi, Nucl. Med. Biol. 30 (2003) 681; g) F. Dieterle, S. Müller-Hagedon, H.M. Liebich, G. Gauglitz, Artif. Intell. Med. 28 (2003) 265.
- [9] a) D.C. Rowley, M.S.T. Hansen, D. Rhodes, C.A. Striffer, H. Ni, J.A. McCammon, F. D. Bushman, W. Fenical, Bioorg. Med. Chem. 10 (2002) 3619; b) A. Arnaud, L. Fontana, A.J. Angulo, Á. Gil, J.M. López-Pedrosa, Clin. Nutr. 22 (2003) 391; c) J.E. Gallant, J. Clin. Virol. 25 (2002) 317.
- [10] a) P. Molina, E. Aller, A. Lorenzo, P. Lopez-Cremades, I. Rioja, A. Ubeda, M. C. Terencio, M.J. Alcaraz, J. Med. Chem. 44 (2001) 1011; b) A. Kumar, S. Sinha, P.M.S. Chauhan, Bioorg. Med. Chem. Lett. 12 (2002) 667.
- [11] M.S. Shingare, B.K. Karale, C.H. Gill, K.N. Gange, M.T. Bachute, Indian J. of Heterocyclic Chem. 9 (1999) 153.
- [12] a) J.-B. Bher, T. Gourlain, A. Helimi, G. Guillermin, Bioorg. Med. Chem. Lett. 13 (2003) 1713; b) H.P. De Koning, M.I. Al-Salabi, A.M. Cohen, G.H. Coombs, J.M. Wastling, Int. J. Paras. 33 (2003) 821; c) J.-B. Behr, T. Gourlain, A. Helimi, G. Guillermin, Bioorg. Med. Chem. Lett. 13 (2003) 1713; d) H.P. De Koning, M.I. Al-Salabi, A.M. Cohen, G. Coombs, J.M. Wastling, Int. J. Paras. 33 (2003) 821.
- [13] D.J. Faulkner, Nat. Product Rep. (1998) 113.
- [14] a) A. Mange, M.V. Merino, C. Sammartin, F.J. Fernandez, M.C. Ochoda, C. Bellver, P. Artigas, F.E. Alvarez, Eur. J. Med. Chem. 24 (1989) 209; b) D.T. Hurst, C. Beaumont, D.T.E. Jones, 92 AKingsly, D., Partridge, J. D., Rutherford, T., J. Aut. J. Chem. 41 (1988) 1209; c) K. Kikuaawa, J. Kato, A. Iwata, Anal. Biochem. 174 (1988) 512; d) J.A. Knight, R.K. Pieper, L. Meclellan, Clin. Chem. 34 (1988) 2433; e) P.W. Albroy, J.T. Corbett, J.L.J. Schroeder, Biochem. Biophys. Methods 13 (1986) 185.
- [15] T. Kata, Japn. Kokai Tokkyo Koho JP. 59 (1984) 974.
- [16] a) Y.S. Sadanandam, M.M. Shetty, P.V. Diwan, Eur. J. Med. Chem. 27 (1992) 87; b) D. Bozong, P. Benko, L. Petocz, M. Szecsey, P. Toempe, G. Gígles, I. Gacsalyi, I. Gyertyan, EGIS Gyozserygyar, Eur. pat. Appl. Ep. 409 (1991) 233; Chem. Abstr., 114 (1991) 247-302z.
- [17] M. Ertan, A. Balkan, S. Sarac, S. Uma, K. Ruebseman, J.F. Renaud, Arzneim-Forsch. 41 (1991) 725.
- [18] B. Springthorpe, A. Bailey, P. Barton, T.N. Birkinshaw, R.V. Bonnert, R.C. Brown, D. Chapman, J. Dixon, S.D. Guile, R.G. Humphries, S.F. Hunt, F. Ince, A.H. Ingall, I. P. Kirk, Bioorg. Med. Chem. Lett. 17 (2007) 6013.
- [19] R. Pontikis, R. Benhida, A.M. Aubertin, D.S. Grierson, C. Monneret, J. Med. Chem. 1997 (1845) 40.
- [20] R.K. Robins, G.R. Revankar, Med. Res. Rev. 5 (1985) 273.
- [21] M. Botta, M. Artico, S. Massa, A. Gambacorta, M.E. Marongiu, A. Pani, P. La Colla, Eur. J. Med. Chem. 27 (1992) 251.
- [22] a) C.O. Kappe, W.M.F. Fabian, Tetrahedron 53 (1997) 2803; b) C.O. Kappe, Eur. J. Med. Chem. 35 (2000) 1043; c) C.O. Kappe, O.V. Shishkin, G. Uray, P. Verdino, Tetrahedron 2000 (1859) 56.
- [23] (a) A.M. Dar, B. Rah, S. Mir, R. Nabi, Shamsuzzaman, M.A. Gatoo, A. Mashrai, Y. Khan, Int. J. Biol. Macromol. 111 (2018) 52-61. (b) A.M. Dar, Shamsuzzaman, M. A. Gatoo, Steroids 104 (2015) 163-175. (c) A.M. Dar, Shamsuzzaman, M.S. Ahmad, Y. Khan, Med. Chem. Res. 26 (2017) 372-383. (d) (c) A.M. Dar, M.A. Gatoo, A. Ahmad, M.S. Ahmad, M.H. Najjar, Shamsuzzaman, J Fluoresc 25 (2015) 1377-1387.
- [24] N. Shahabadi, S. Khashanian, M. Khosravi, M. Mahdavi, Transit. Met. Chem. 35 (2010) 699-705.
- [25] A.J. Berk, TBP-like factors come into focus, Cell 103 (2000) 5-8.
- [26] A. Wolfe, G.H. Shimer, T. Meehan, A. Wolfe, G.H. Shimer, T. Meehan, Biochemistry 26 (1987) 6392-6396.
- [27] L.F. Tan, H. Chao, K.C. Zhen, J.J. Fei, F. Wang, Y.F. Zhou, L.N. Ji, Polyhedron 26 (2007) 5458-5468.
- [28] G. Scatchard, Ann. N. Y. Acad. Sci. 51 (1949) 660-672.
- [29] E. Trotta, G. Del, N. Erba, M. Paci, Biochemistry 39 (2000) 6799-6808.
- [30] P. Wittung, P. Nielsen, B. Norden, J. Am. Chem. Soc. 118 (1996) 7049-7054.
- [31] A.M. Dar, Z. Shamsuzzaman, K. Yaseen, A. Alam, M.A. Gatoo Hussain, J. Mol. Struct. 1045 (2013) 62-71.
- [32] C.E.B. Smith, M.S. Searle, Nucl. Acids Res. 27 (1999) 1619-1624.
- [33] P.U. Maheswari, M. Palaniandavar, J. Inorg. Biochem. 98 (2004) 219-230.
- [34] S. Satyanarayana, J.C. Dabrowiak, J.B. Chaires, Biochemistry 31 (1992) 9319-9324.
- [35] I. Haq, J. Ladbury, J. Mol. Recognit. 13 (2000) 188-197.
- [36] T. Mosmann, J. Immunol. Methods 65 (1983) 55-63.
- [37] G.S. Son, J. Am. Chem. Soc. 120 (1998) 6451-6457.
- [38] Shamsuzzaman, A. Salim, M. Aslam, F. Naqvi, Synth. Commun. 27 (1997) 2171-2175.
- [39] M.E. Reicmann, S.A. Rice, C.A. Thomas, P. Doty, J. Am. Chem. Soc. 76 (1954) 3047-3053.
- [40] A.M. Shamsuzzaman, Y. Dar, A. Khan, J. Sohail, Photochem. Photobiol. B Biol. 129 (2013) 36-47.
- [41] R. Vijayalakshmi, M. Kanthimathi, V. Subramanian, B.U. Nair, Biochim. Biophys. Acta 1475 (2000) 157-162.
- [42] D. Mustard, D.W. Ritchie, Proteins: Struct., Funct., Bioinf. 60 (2005) 269-274.
- [43] D.L. Spector, R.D. Goldman, L.A. Leinwand (Eds.), Cells: A Laboratory Manual, vol. 1, Cold Spring Harbour Laboratory Press: New York, NY, 1998, Ch. 15.
- [44] M.J. Frisch, G.W. Trucks, H.B. Schlegel, G.E. Scuseria, M.A. Robb, J.R. Cheeseman, G. Scalmani, V. Barone, B. Mennucci, G.A. Petersson, H. Nakatsuji, M. Caricato, X. Li, H.P. Hratchian, A.F. Izmaylov, J. Bloino, G. Zheng, J.L. Sonnenberg, M. Hada, M. Ehara, K. Toyota, R. Fukuda, J. Hasegawa, M. Ishida, T. Nakajima, Y. Honda, O. Kitao, H. Nakai, T. Vreven, J.A. Montgomery Jr., J.E. Peralta, F. Ogliaro, M. Bearpark, J.J. Heyd, E. Brothers, K.N. Kudin, V.N. Staroverov, R. Kobayashi, J. Normand, K. Raghavachari, A. Rendell, J.C. Burant, S.S. Iyengar, J. Tomasi, M. Cossi, N. Rega, J.M. Millam, M. Klene, J.E. Knox, J.B. Cross, V. Bakken, C. Adamo, J. Jaramillo, R. Gomperts, R.E. Stratmann, O. Yazyev, A.J. Austin, R. Cammi, C. Pomelli, J.W. Ochterski, R.L. Martin, K. Morokuma, V.G. Zakrzewski, G.A. Voth, P. Salvador, J.J. Dannenberg, S. Dapprich, A.D. Daniels, O. Farkas, J.B. Foresman, J. V. Ortiz, J. Cioslowski, D.J. Fox, Gaussian 09, Revision D.01, Gaussian Inc, Wallingford CT, 2009.
- [45] S. Grimme, Semiempirical GGA-type density functional constructed with a long range dispersion correction, J. Comput. Chem. 27 (2006) 1787-1799.
- [46] M. Ansari, N. Vyas, A. Ansari, G. Rajaraman, Oxidation of methane by an N-bridged high valent diiron-oxo species: electronic structure implications on the reactivity, Dalton Trans. 44 (2015) 15232-15243.